



## TRUE SOURCES OF LINEAR SOUND IN PLANE COUETTE FLOW

### Jan-Niklas Hau & Martin Oberlack

Department of Fluid Mechanics  
TU Darmstadt  
Petersenstr. 30, 64287 Darmstadt, Germany  
Graduate School CE, TU Darmstadt  
Dolivostraße 15, 64293 Darmstadt, Germany  
hau@fdy.tu-darmstadt.de

### George Chagelishvili

Abastumani Astrophysical Observatory  
Ilia State University  
Tbilisi 0160, Georgia  
M. Nodia Institute of Geophysics  
Tbilisi State University  
Tbilisi 0128, Georgia  
g.chagelishvili@astro-ge.org

### George Khujadze

Chair of Fluid Mechanics  
University Siegen  
Paul-Bonatz-Str. 9-11, 57068 Siegen, Germany  
Abastumani Astrophysical Observatory,  
Ilia State University  
Tbilisi 0160, Georgia  
george.khujadze@uni-siegen.de

### Alexander Tevzadze

Faculty of Exact and Natural Sciences  
Javakhishvili Tbilisi State University  
Tbilisi 0128, Georgia  
aleko@tevza.org

### ABSTRACT

The sound generation by pure vortex mode disturbances in an two-dimensional (2D) unbounded inviscid plane Couette flow is investigated. We present results by Kelvin-mode analysis as well as numerical simulations of the Euler equations, while focusing on the dynamics in the spectral plane. Our results show a dominance of the anisotropic linear sound generation in subsonic shear flows by vortices inside the boundaries of rapid distortion theory (RDT). The linearly generated, highly directional field is comparable to the hydrodynamic field, which physical headstone is the mode coupling, induced by the non-normality in shear flow systems at moderate shear rates of the velocity. Comparisons of the classical acoustic analogy (AA) approach by Lighthill (1952) with the herein presented results identify the inability of AAs to capture the shear-induced anisotropy of the generated waves in the spectral plane.

### INTRODUCTION

Aerodynamic sound generation is a major subject of fluid dynamics, with applications in wide areas of engineering problems, even extending to the astrophysical context (helio- and astroseismology). The framework for modern aero-acoustic research has been accomplished by Lighthill's pioneering work (Lighthill, 1952) and the derivation of an AA. According to Lighthill (1954) the linear sound generation can be increased by a mean shear flow, due to the linear terms in the source term,  $\mathcal{S}$ . This statement motivates our present research, having the dual purpose of: (i) rethinking Lighthill's approach Lighthill (1952, 1954) in the light of the breakthrough of the hydrodynamic stability community in the 1990s (e.g. Chagelishvili *et al.* (1997b);

Schmid & Henningson (2001) and references herein) that has been followed by the understanding of phenomena introduced by the non-normality of non-uniform flow systems; (ii) comparing the efficiency of the linear and non-linear mechanisms of aerodynamic sound generation at different Mach numbers,  $\mathcal{M}$ , and RDT parameters,  $\mathcal{D}$ , of the embedded flow eddies. In shear flows the set of governing equations, describing the linear dynamics, are non-normal, hence, likewise the operators in the mathematical formalism of the modal analysis, while the corresponding eigenmodes are non-orthogonal (e.g. Schmid & Henningson (2001)). This leads to strong interference phenomena among the eigenmodes, which are not captured by the classic modal analysis, but can be circumvented by the non-modal approach. The presented results have been obtained by means of Kelvin-mode analysis and numerical simulations of the Euler equations. By focusing on the dynamics in the spectral plane, it is possible to grasp the basic physics of wave generation by initially pure vortex perturbations embedded in a 2D, inviscid and unbounded plane Couette flow. This is characterised by a homogeneous shear of velocity ( $\mathbf{U}_0 = (Ay, 0)$ ), shear parameter  $A > 0$  without the loss of generality), uniform pressure and density distribution.

By the chosen approach we assure to centre our attention on phenomena induced by the non-normal nature of the base flow system, partially appearing in jets, too, thus, shedding some light on the open question for the *true sources* of aerodynamic sound, which are not properly defined until now, (Goldstein, 2005).

### KELVIN MODE ANALYSIS

First of all we capture the generation of wave modes from single vortex Kelvin modes by employ-

ing a non-normal approach. The basis of the applied Kelvin mode approach is represented by the transformation of the 2D linearised Euler equations (LEE) about the uniform shear flow, with  $\mathbf{U}_0 = (Ay, 0)$ , in a co-moving frame. The standard procedure of non-modal analysis subsequently employs the spatial Fourier expansion of the perturbations with a constant streamwise,  $k_x$ , and a time-dependent cross-stream wavenumber  $k_y(\tau) = k_y(0) - k_x A \tau$ :  $\Psi = \hat{\Psi} \exp(ik_x x + ik_y(\tau)y)$ , with  $\Psi = \{u_x(\mathbf{x}, \tau), u_y(\mathbf{x}, \tau), \rho(\mathbf{x}, \tau)/\rho_0\}$  and  $\hat{\Psi} = \{v_x(\mathbf{k}, \tau), v_y(\mathbf{k}, \tau), D(\mathbf{k}, \tau)\}$ , where  $\{u_x, u_y, \rho/\rho_0\}$  and  $\{v_x, v_y, D \equiv i\rho/\rho_0\}$  denote the stream- and cross-streamwise velocity and normalised density perturbations in physical ( $\mathbf{x} = (x, y)$ ) space and of the perturbation spatial Fourier harmonics (SFH), respectively, with  $\mathbf{k} = (k_x, k_y)$ . The time dependence appearing in  $k_y(\tau)$  is due to the shearing background. The set of the LEE for the SFH thence reduces to the following form:

$$\begin{aligned} \frac{dv_x}{d\tau} &= -Av_y - k_x c_s^2 D \\ \frac{dv_y}{d\tau} &= -k_y(\tau) c_s^2 D, \quad \frac{dD}{d\tau} = k_x v_x + k_y(\tau) v_y. \end{aligned} \quad (1)$$

Eqs. (1) are characterised by the essential time-invariant  $\mathscr{W}$

$$k_y(\tau) v_x - k_x v_y + AD \equiv \mathscr{W}. \quad (2)$$

This corresponds to the fact that  $\mathscr{W}$ , the *potential vorticity*, is a conserved quantity ( $d\mathscr{W}/d\tau = 0$ ) and plays a crucial role in the rigorous identification/definition of perturbation modes in this peculiar shear flow. By re-combining Eqs. (1) including the potential vorticity as a key-variable, one way to reduce Eqs. (1) to a second order inhomogeneous differential equation for  $v_x(\tau)$  is given by

$$\left[ \frac{d^2}{d\tau^2} + \omega^2(\tau) \right] v_x(\tau) = c_s^2 k_y(\tau) \mathscr{W}, \quad (3)$$

where  $\omega^2 = c_s^2(k_x^2 + k_y^2(\tau))$ . This equation can be interpreted as the spectral form of the AA equations in the linear limit, as it has the form of a wave-equation with a time-dependent frequency  $\omega$  and a *physical* source term on the right-hand side (RHS). From the physical point of view, Eq. (3) describes two different modes/types of perturbations: (i) acoustic wave modes ( $v_x^{(w)}$ ) that are described by the general solution of the corresponding homogeneous equation and (ii) vortex modes ( $v_x^{(v)}$ ) that are aperiodic, originated from the equation inhomogeneity, ( $k_y(\tau)\mathscr{W}$ ). The latter are associated with the particular solution of the inhomogeneous equation (the amplitude of the vortex mode is proportional to  $\mathscr{W}$ , hence goes to zero when  $\mathscr{W} = 0$ ).

### A linear mechanism of wave generation by vortices

By imposing a pure vortex mode SFH into the shear flow, a distinct linear mechanism of acoustic wave generation is found. This is due to the (vortex and wave) mode coupling, induced by the non-normality of the shear flow system and efficient at moderate/high Mach numbers of the initially embedded perturbation,  $\mathcal{M} = A/(k_x c_s) \gtrsim 0.3$ ,

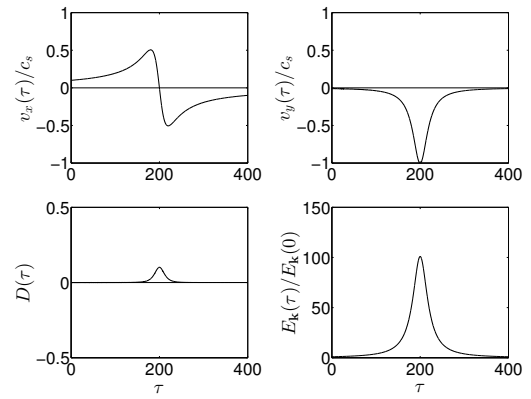


Figure 1: Evolution of initially pure vortex SFH in terms of normalised velocity and density perturbations ( $v_x(\tau)/c_s$ ,  $v_y(\tau)/c_s$  and  $D \equiv i\rho(\tau)/\rho_0$ ) and its normalised energy ( $E_{\mathbf{k}}(\tau)/E_{\mathbf{k}}(0)$ ) at  $\mathcal{M} = 0.05$ , and  $k_{y0}/k_x = 10$ .

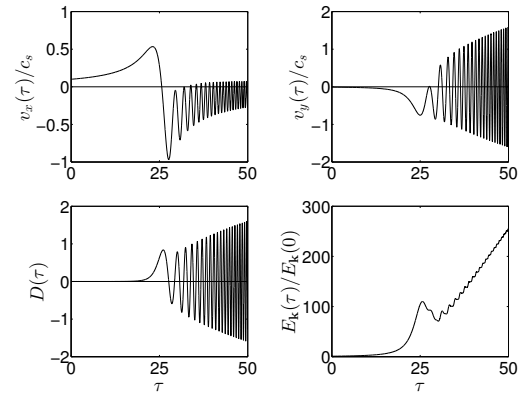


Figure 2: The same as for Fig. 2 at  $\mathcal{M} = 0.40$  – wave generation appears at times  $\tau = \tau^* = k_{y0}/(Ak_x)$ .

(Chagelishvili *et al.*, 1997a). Although  $k_x$  is constant in time in the linear limit, nonlinear effects might redistribute the modes also in streamwise direction. In order to visualise the aforementioned wave generation phenomenon, numerical calculations of Eqs. (1) are carried out for initially imposed pure vortex SFH (without admixes of acoustic waves) that satisfy the condition  $k_{y0}/k_x > 0$  at  $\tau = 0$ , with  $k_{y0} = k_y(0)$  and are presented in Fig. 1 and Fig. 2, respectively. The extraction of pure vortex mode SFH is accomplished by a numerical procedure, which is based on the WKB (Wentzel, Kramers, Brillouin) (Nayfeh, 2000) approximation in the adiabatic limit of the perturbations ( $|k_y/k_x| \gg 1$ ). We concentrate our attention on  $\mathcal{M} \lesssim 1$  in order to avoid any appearances of shock waves.

Whereas for low values of  $\mathcal{M}$  (see Fig. 1) there is no indicator for wave emergence and the vortex mode behaves as in the incompressible limit, it appears that the generation of acoustic waves by vortices takes place at the moment of the SFH crossing the line of  $k_y = 0$  for higher values of  $\mathcal{M}$ , Fig. 2. The moment of wave emergence corresponds to the critical time  $\tau^* = k_{y0}/(Ak_x)$ .

The effective parameter of acoustic wave generation with  $\tau_{\pm}^* = \tau^* \pm 0$  can be defined as

$$\eta \equiv \frac{E_{\mathbf{k}}^{(w)}(\tau_{+}^*)}{E_{\mathbf{k}}^{(v)}(\tau_{-}^*)} = \frac{4v_x^2(\tau^*)}{v_x^2(\tau^*) + v_y^2(\tau^*) + c_s^2 D^2(\tau^*)}, \quad (4)$$

wherein the energetic parts of the regarded mode – vortex

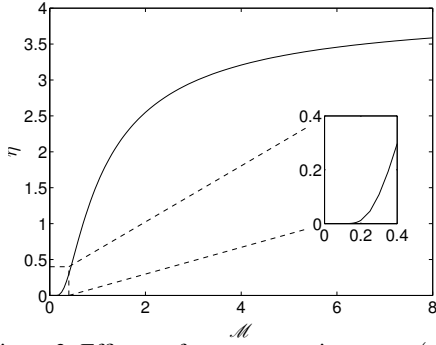


Figure 3: Efficacy of wave-generation  $\eta = \eta(\mathcal{M})$ .

(v) and wave (w) part – are

$$\begin{aligned} E_{\mathbf{k}}^{(v)}(\tau < \tau^*) &\equiv \frac{\rho_0}{2} \left[ v_x^{(v)2} + v_y^{(v)2} + c_s^2 D^{(v)2} \right] \\ E_{\mathbf{k}}^{(w)}(\tau > \tau^*) &\equiv \frac{\rho_0}{2} \left[ v_x^{(w)2} + v_y^{(w)2} + c_s^2 D^{(w)2} \right]. \end{aligned} \quad (5)$$

Naturally,  $E^{(v)}$  and  $E^{(w)}$  do not have any physical meaning in the energy gaining region,  $|k_y(\tau)/k_x| \lesssim 1$ , where vortex and wave SFHs strongly interfere. They, however, get the described meaning, when  $\mathcal{M}^*(\tau) = A/\omega(\tau) \ll 1$  and the mode interference is negligible, which is true in the adiabatic limit. The RHS of Eq. 4 is recovered by symmetry properties of the primitive variables. Numerically evaluating Eq. (4) as a function of  $\mathcal{M}$ , the result is presented in Fig. 3, where the inner plot shows a magnified view of the area of  $\mathcal{M} \in [0, 0.4]$ .

Obviously, the generation of waves becomes noticeable around  $\mathcal{M} = 0.2$ , substantial at  $\mathcal{M} = 0.3$ , while asymptotically aspiring towards a value of  $\lim_{\mathcal{M} \rightarrow \infty} \eta = 4$ . The cause of the actual absence of the wave generation phenomenon at low shear rates is not the existence of a certain threshold, but the fact that  $|v_x(\tau^*)|$  is largely reduced at  $\mathcal{M} < 0.1$ . The calculations, thence, show that the value of the Mach number drastically changes the vortex dynamics and their potential of wave emergence. Consequently, introducing vortex and wave characteristics at  $\tau \rightarrow \tau_+^*$  and evaluating their dynamics, we can asymptotically determine values of the physical quantities of the SFHs (at  $\mathcal{M}^*(\tau) \ll 1$ ). Our numerical calculations show that  $E^{(w)}(\tau)$  increases and  $E^{(v)}(\tau)$  decreases asymptotically in time. Thus the single wave SFH, generated at  $\tau = \tau^*$ , amplifies by gaining energy from the surrounding shear flow at times  $\tau \geq \tau^*$ . The vortex SFH, instead, gives its energy back to the background flow and diminishes in time.

At time  $\tau_+^*$ , we only have vortex SFH, which energy is defined by the first part of (5). From this equation and from the symmetry properties of vortex SFHs we derive that

$$E_{\mathbf{k}}(\tau_-^*) \equiv E_{\mathbf{k}}^{(v)}(\tau_-^*) \quad \text{and} \quad E_{\mathbf{k}}^{(v)}(\tau_-^*) = E_{\mathbf{k}}^{(v)}(\tau_+^*), \quad (6)$$

i.e. the vortex energy at time  $\tau_+^*$  is equal to the energy of the vortex SFH at time  $\tau_-^*$ , independent from the value of the generated wave SFH amplitude. Hence, we can conclude that the dynamics of the vortex SFH does not depend on the amplitude of the generated wave SFH. The emerged wave SFH, thus, does not change the vortex SFH energetics and is energetically supplied by the shear flow and it is feasible to state that the vortex SFH acts as a mediator between the background flow and the wave SFH at  $\tau^*$ .

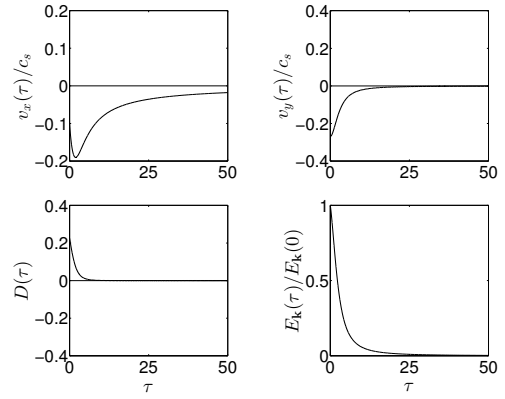


Figure 4: The same as for Fig. 2 for  $k_{y0}/k_x = -10^{-5}$ .

For the reason that  $\tau^*$  cannot be reached for SFHs initially located in regions of  $|k_y/k_x| < 0$ , vortical perturbations here do not inhere the potential to trigger wave-emergence. This fact is striking and illustrated in Fig. 4 and of major importance, because it underlines that the linearly generated acoustic waves are anisotropic in the  $(k_x, k_y)$ -plane and, consequently, also in the physical one. Additionally, the fact that the cross-stream wavenumber of each wave harmonic is zero,  $k_y(\tau^*) = 0$  (irrespective of the value of  $k_x$ ), at the moment of wave emission by the related vortex SFH, leads to a narrow emission-angle of linearly generated waves and innately distinguishes them from the wide-angle modes of nonlinearly generated waves.

## DIRECT NUMERICAL SIMULATIONS

Fully nonlinear numerical simulations of the Euler equations are carried out that serve as a tool for the identification of further appearing more complex nonlinear phenomena and as a supplementary basis for the analytic results presented above, substantiating the importance of the linear sound generating mechanism in uniform shear flows.

### Numerical setup

We carry out numerical ideal hydrodynamic simulations using the well tested code PLUTO. The code was developed for the solution of (hypersonic) flows in one, two and three spatial dimensions and different systems of coordinates (Mignone *et al.*, 2007). It provides a multiphysics, multialgorithm modular environment. Different hydrodynamic modules and algorithms may be independently selected to properly describe Newtonian, relativistic, magnetohydrodynamics, or relativistic magnetohydrodynamics fluids. In our case, Newtonian hydrodynamics have been used, which module implements the equations of classical inviscid fluid dynamics with an ideal equation of state (Euler equations). The modular structure exploits a general framework for integrating a system of conservation laws, built on modern Godunov-type shock-capturing schemes. For our simulations a piecewise-parabolic-method is employed as implemented by Colella & Woodward (1984), having a fourth-order accuracy on a uniform mesh, together with the third-order Runge-Kutta method in time.

The domain of our numerical simulations is chosen as a box extending from  $-L$  to  $L$ , with  $L = 10$ , in each direction, and a number of  $N_x \times N_y = 8192^2$  equidistantly distributed zones in  $x$ - and  $y$ -direction. This leads to a grid spacing

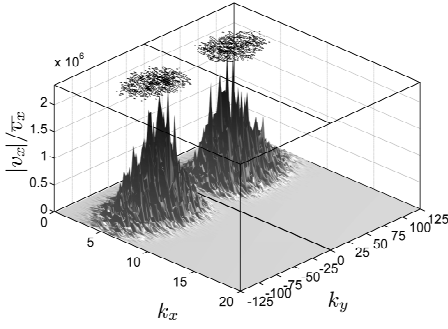


Figure 5: Initially imposed normalised (absolute) streamwise velocity disturbance distribution in the spectral plane.

of  $\Delta x = \Delta y = 0.0024$  in the physical plane, which is sufficient for the range of wavenumbers we are interested in, gearing to the suggestion of Tam (2004) that the following estimation holds:  $N = N_\lambda L / \pi k_{\max}^*$ , where  $k_{\max}^*$  is the maximal wavenumber we are interested in, and  $N_\lambda$  is the number of points per smallest wavelength, which is conservatively estimated to 20. This approach is due to the assumption that the processes of primary interest in this research appear around small values of  $|\mathbf{k}| \leq 150$ . The properties in spectral space can be summarised as follows:  $k_{\min} = 2\pi/(2L) \approx 0.314$  and  $k_{\max} = 2\pi/(2L) \cdot (N - 1) \approx 2573$ , hence  $\mathbf{k} \in [-k_{\max}/2, k_{\max}/2]$  with  $\Delta k = k_{\min}$ , equally, in  $k_x$ - and  $k_y$ -direction. Further, we employ periodic boundary conditions in  $x$ -direction, while outflow boundary conditions are employed in  $y$ -direction.

### Initial conditions

In order to highlight the effectiveness of the linear and nonlinear wave generation mechanisms, the initially imposed disturbances have a specific spectrum, which is given for the streamwise velocity disturbance,  $v_x(\mathbf{x}, 0)$ , by

$$v_x(\mathbf{x}, 0) = B e^{-\left(\frac{y}{2L-d}\right)^4} \int_{\mathbf{k}} \frac{k_y^2}{\Delta k_y^2} e^{-\left[\left(\frac{k_x - k_{x0}}{\Delta k_x}\right)^2 + \left(\frac{k_y}{\Delta k_y}\right)^2\right]} 2\pi i \zeta_p(\mathbf{k}) \zeta_a(\mathbf{k}) e^{i\mathbf{k} \cdot \mathbf{x}} d\mathbf{k}. \quad (7)$$

Here,  $\zeta_a(\mathbf{k})$ ,  $\zeta_p(\mathbf{k}) \in [0, 1]$  are random numbers and impart a stochastic nature to the disturbances.  $L$  and  $d$  denote the box-size and localisation scale in  $y$ -direction. The disturbance-spectrum is localised in the  $(k_x, k_y)$ -plane with half-widths  $\Delta k_x$  and  $\Delta k_y$  along the  $k_x$ - and  $k_y$ -axis, respectively, while centred around the initial streamwise wavenumber  $k_{x0}$ . Herein, it is sufficient to introduce only a streamwise velocity disturbances spectrum, as the remaining quantities,  $v_y$  and  $\rho$ , can be recovered numerically. This provides the uniquely associated physical quantities for an arbitrary chosen spectrum of  $v_x$  of pure vortex mode SFHs, which is presented in Fig. 5 in the  $(k_x, k_y)$ -plane with superimposed contours in the upper region, normalised on

$$\bar{\Psi} = \sqrt{\frac{1}{N_x N_y} \iint d\mathbf{k} |\hat{\Psi}(k_x, k_y, 0)|^2}. \quad (8)$$

Herein, we have chosen the following set of parameters:  $A = 4$ ,  $k_{x0} = 5$ ,  $\Delta k_x = 2$ ,  $\Delta k_y = 50$  and  $d = 2$ . The values of  $k_{x0}$ ,  $\Delta k_x$  and  $\Delta k_y$  are chosen in such a way to ensure transient amplification of the disturbance SFHs. Thus,

$\mathcal{M} = 0.8$  and excessive wave emergence can be expected at the critical time of the main bulk of disturbance modes (see Fig. 3). Simultaneously,  $k_{x0} > \Delta k_x$  in order to allow an easy distinction between linearly and nonlinearly generated acoustic waves. The former should appear around  $k_{x0}$  due to the described drift of SFHs along the  $k_y$ -axis, while the latter are expected to appear around  $2k_{x0}$ . By the chosen value of  $d$  we can follow the generation of acoustic waves by vortices for a sufficient time period, which are initially stochastically distributed, yet, confined in  $y$ -direction.

For the aimed efficiency comparison of linear and nonlinear sound generation it is suitable to introduce a distortion parameter ( $\mathcal{D}$ ) (Simone *et al.*, 1997) as  $\mathcal{D} = A/k_{x0}q$ , where  $q^2/2$  is the turbulent kinetic energy of the largest energy containing scales, which are located around  $k_x \approx k_{x0}$ . As  $\mathcal{D}$  is a function of  $B$  that determines the initial disturbance amplitude (see Eq. (7)), it is convenient to compare linearly and nonlinearly generated sound by the choice of  $\mathcal{D}$ . Of course, the lower the value of  $\mathcal{D}$  (higher  $B$ ) the stronger is the influence of nonlinear effects. We restrict ourselves to  $\mathcal{D} \gtrsim 1$ , in which range RDT is still assumed to be a good approximation of the active processes (Batchelor & Proudman, 1952), and linear processes are expected to play a major role. (Lighthill, 1952).

The two subsequently presented cases are both run at a moderate Mach number ( $\mathcal{M} = 0.8$ ), whereas  $B = 1 \cdot 10^3$ ;  $6 \cdot 10^5$  and Case 1:  $\mathcal{D} = 1000$ ; Case 2:  $\mathcal{D} = 1$  respectively.

### Results

As 2D perturbations are not self-sustaining by definition, we follow the dynamics of the vortex density disturbances and their conversion into wave ones (VD and WD, respectively), during a confined time interval. Further, we stop the numerical simulations, as soon as the generated waves reach the outflow boundaries in  $y$ -direction, in order to avoid any numerical problems of spurious reflections.

**Case 1** Regarding Case 1 ( $\mathcal{D} \simeq 1000$ ), which we suppose to be dominated by linear mechanisms, it is possible to track the disturbance dynamics in the spectral half plane, as presented in Fig. 6.

It becomes evident that each disturbance SFH drifts along the  $k_y$ -axis, with a drift velocity proportional to  $k_x$ . As the disturbance consist initially solely of VD, SFHs located in the region of  $k_y/k_x < 0$  immediately attenuate (see panels (b)-(c) and compare with Fig. 4), whereas SFHs located in regions of  $0 < k_y/k_x < 1$ , transiently amplify (panels (a)-(c)). Only these SFHs bear the potential to amplify and, *ergo*, to generate waves at the moment of crossing the line of  $k_y = 0$ . As attenuation of VD SFHs located in the region  $k_y/k_x < 0$  starts immediately, it is possible to state that any (remaining) SFHs in this region are of wave nature at times  $\tau > 0.6$  and linearly generated. This is underlined by the wave-like pattern, as presented in the framework of the linear analysis (Fig. 2), which especially becomes evident for later times, panels (d)-(f), when the waves draw energy from the base flow. The bulk of VD SFHs exceeds their critical time in panel (e). Of course, till this stage numerous VD SFHs have crossed the  $k_x$ -axis, hence, have passed through the sequence following *linear* processes, consisting of (i) drift of all kind of perturbations; (ii) transient growth of vortex mode SFH; (iii) generation of acoustic wave SFH by vortex ones; (iv) algebraic amplification of wave SFH, yet, with less time for transient amplification. *Ergo* the waves linearly generated by the VD SFH bulk are

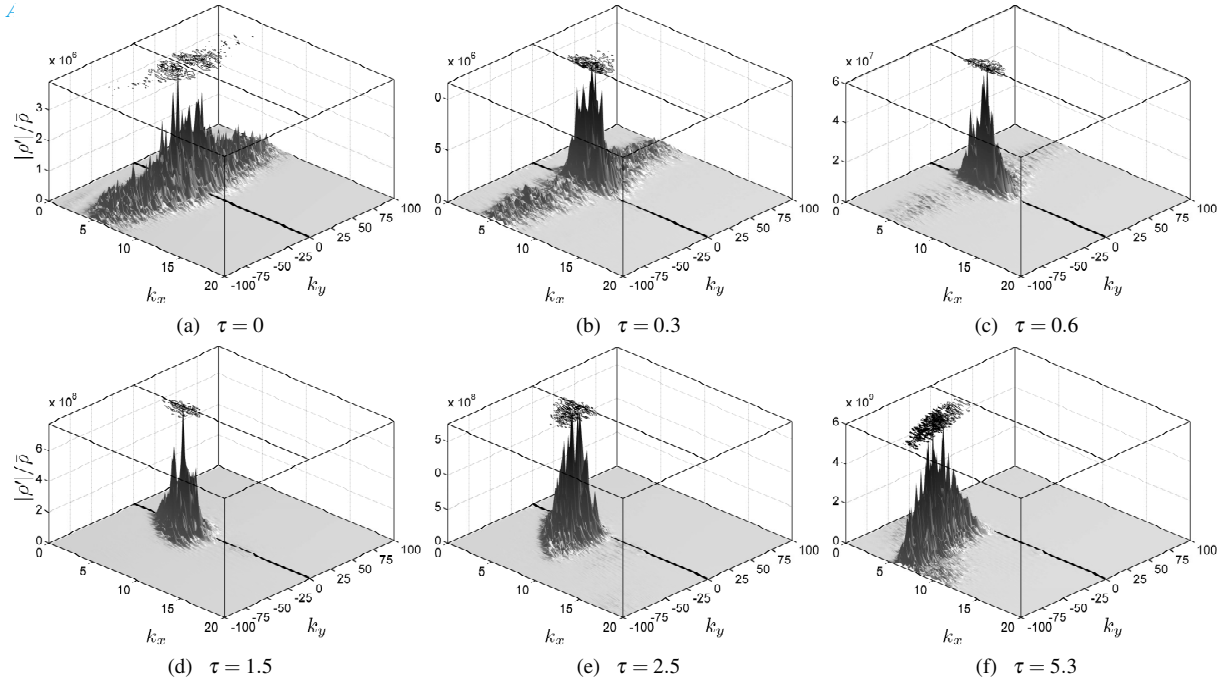


Figure 6: Evolving density perturbations for initially pure vortex mode perturbations in the  $(k_x, k_y)$ -plane at different times in terms of absolute density disturbance amplitudes, normalised on the absolute mean-value of initial density perturbations  $\bar{\rho}$  for  $\mathcal{D} \simeq 1000$ .

more pronounced. During the drift of the newly generated waves along the  $k_y$ -axis, they gain energy from the mean flow, amplify but stay confined in the spectral plane. Their amplitudes become large enough to start nonlinear wave-wave interactions. Thus, the thereby resulting SFHs appear around  $k_x = 2k_{x0} = 10$  for larger times, panel (f). Still, their amplitude is so small that they can be labelled as inferior to the linearly generated waves.

Finally, we can exclude either nonlinear vortex-vortex and vortex-wave interactions, as all VD SFHs have become ineffective in comparison to the WD SFHs.

**Case 2** The sequence of plots in Fig. 7 represents the dynamics of the normalised density perturbations for  $\mathcal{D} \simeq 1$ . The comparably high initial perturbation amplitude (at the border of RDT validity) causes immediate nonlinear interactions of VD modes with each other. This leads to the appearance of additional VD perturbations around  $k_x \approx 2k_{x0}$  (panel (b)). The amplitude of those nonlinearly generated VD mode disturbances exceed the linearly assigned ones after a comparably short period of time (panel (c)). Although, partially nonlinearly generated, all VD perturbations undergo the described drift in the  $\mathbf{k}$ -plane and subsequently amplify, presupposed they are located in regions of  $k_y/k_x > 0$  (see Fig.2 and 4). The ones situated in regions of  $k_y/k_x < 0$  immediately attenuate, without the potential of wave-generation. These results are identical to the ones obtained for the Case 1. Yet, the nonlinearly generated vortex SFHs (located around  $k_x \approx 2k_{x0}$ ) have a smaller Mach number,  $\mathcal{M} \approx 0.4$ , and generate acoustic wave SFHs in a weaker manner. So, while weakly generating waves, they themselves disappear by drifting in regions of  $k_y/k_x < 0$  (see (d)). This is a compelling indicator for the omnipresence of the linear mechanisms, acting even on nonlinearly generated disturbances. In this particular panel nonlinear processes clearly dominate the dynamical picture. Yet, it is visible that the linear ones do not become negligible due to the former described sequence of linear pro-

cesses. This chain of processes is inevitably connected to the spectral drift of the perturbations (WD and VD type), whereas the hereby created wave modes mix with vortex ones as seen in panel (e). On the other hand the perturbations in panel (f) mostly have wave nature, as VD modes are almost solely generated by interactions with themselves. Clearly, the generation of waves by vortex-vortex interactions, such as analysed by Lighthill (1952), is inferior, in favour that the generation by vortices is the dominating part of these two. Together with the observation that the nonlinear generation of vortex SFHs by wave disturbances is rather negligible our results perfectly coincides the view of Chu & Kovásznyai (1958), claiming that the solenoidal disturbance components play no part in the generation of wave modes, yet, are seen as the basis of the energy transfer between different sized eddies.

### Comparison with Lighthill's source term

As we compare the observed specificity of the linear sound generation mechanism by vortices with the linearly (l) and nonlinear (nl) predicted sources of sound by Lighthill (1952),  $\mathcal{S} = \mathcal{S}_l + \mathcal{S}_{nl}$ , linearised about the described base flow, it becomes evident that linear sources are predicted in all quadrants of the  $(k_x, k_y)$ -plane as presented in Fig. 8(a), whereas (b) nonlinear generated sound is predicted around  $k_x \approx 2k_{x0}$  and  $k_x \approx 0$ . The reason for the inherent misleading result by the AA representation is found in its incapability to take the described anisotropy into account. Obviously, vortices only inhere the *potential* of linear wave excitation. So, our results clearly show a failure of the AA approach and thereby support Goldstein (2005), who claims that this very approach is unsuitable to identify the *true sources* of aerodynamically generated sound, rather than as a modelling framework. The fundamental character of the failure is unambiguously connected to phenomena induced by the the non-normality of nonuniform flow systems and makes it (for many applications) unfeasible to remain in the framework of the AA "ideology".

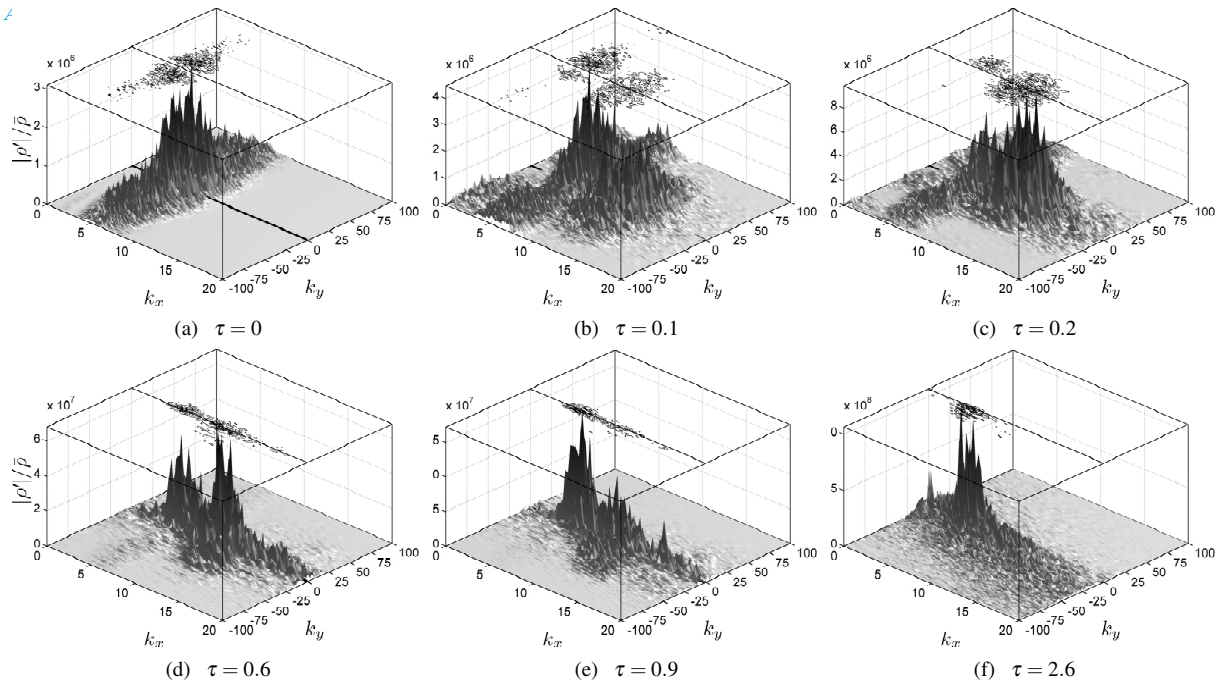


Figure 7: The same as for Fig. 6 for  $\mathcal{D} \simeq 1000$ .

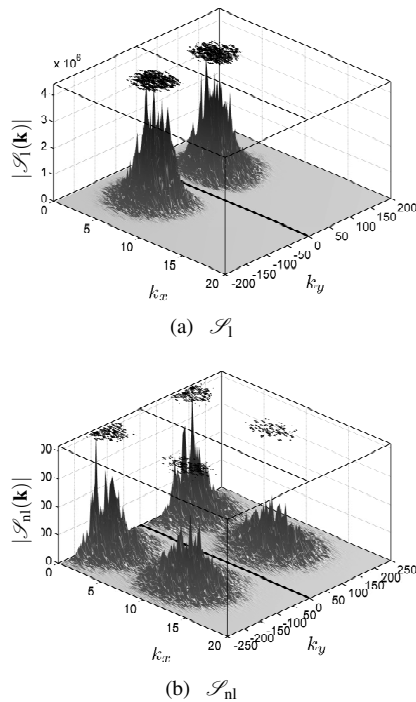


Figure 8: Lighthill's spectral source term prediction

## CONCLUSION

Analysing the complexity of linear/nonlinear processes involved in (i) the generation and (ii) further propagation of acoustic waves in the flow by vortices in spectral space, our research reveals a failure of the representation of the anisotropic linear sound generation mechanism by Lighthill's AA formulation and a dominance of the linear processes inside the boundaries of RDT. Thereby, the omnipresence of the spectral drift is eye-catching and shows the significance of the linear processes in non-normal flow systems, even acting on nonlinearly generated SFHs and, thus, must not be underestimated.

## REFERENCES

- Batchelor, G. K. & Proudman, I. 1952 The effect of rapid distortion of a fluid in turbulent motion. *Quart. J. Mech. Appl. Math.* **7**, 83–103.
- Chagelishvili, G. D., Khujadze, G. R., Lominadze, J.G. & Rogava, A. D. 1997a Acoustic waves in unbounded shear flows. *Phys. Fluids* **9**, 1955–1962.
- Chagelishvili, G. D., Tevzadze, A.G., Bodo, G. & Moiseev, S. S. 1997b Linear mechanism of wave emergence from vortices in smooth shear flows. *Phys. Rev. Lett.* **79**, 3178–3181.
- Chu, B.-T. & Kovásznyai, L. S. G. 1958 Non-linear interactions in a viscous heat-conducting compressible gas. *J. Fluid Mech.* **3**, 494–514.
- Colella, P. & Woodward, P. R. 1984 The piecewise parabolic method (PPM) for gas-dynamical simulations. *J. Comput. Phys.* **54**, 174–201.
- Goldstein, M. E. 2005 On identifying the true sources of aerodynamic sound. *J. Fluid Mech.* **526**, 337–347.
- Lighthill, M. J. 1952 On sound generated aerodynamically – I. General theory. *Proc. Roy. Soc. London Ser. A* **211**, 564–587.
- Lighthill, M. J. 1954 On sound generated aerodynamically – II. Turbulence as a source of sound. *Proc. Roy. Soc. London Ser. A* **222**, 1–32.
- Mignone, A., Bodo, G., Massaglia, S., Matsakos, T., Tesileanu, O., Zanni, C. & Ferrari, A. 2007 PLUTO: A numerical code for computational astrophysics. *Astrophys. J. Suppl. Ser.* **170**, 228–242.
- Nayfeh, A. H. 2000 *Perturbation Methods*. Wiley-VCH.
- Schmid, P. J. & Henningson, D. S. 2001 *Stability and Transition in Shear Flows*. Applied Mathematical Sciences Bd. 142. Springer.
- Simone, A., Coleman, G. N. & Cambon, C. 1997 The effect of compressibility on turbulent shear flow: A Rapid-Distortion-Theory and direct-numerical-simulation study. *J. Fluid Mech.* **330**, 307–338.
- Tam, C. K. W. 2004 Computational aeroacoustics: An overview of computational challenges and applications. *Int. J. Comput. Fluid D.* **18**, 547–567.